Supplementary information

Valley-enhanced fast relaxation of gate-controlled donor qubits in silicon

Péter Boross,[1] Gábor Széchenyi,[1] and András Pályi[2]

[1] *Institute of Physics, Eötvös University, Budapest, Hungary*

[2] *Department of Physics and MTA-BME Condensed Matter Research Group, Budapest University of Technology and Economics, Budapest, Hungary*

(Dated: May 4, 2016)

I. OVERLAPS GOVERNING FLIP-FLOP RELAXATION

One key ingredient governing the flip-flop relaxation rates is the level of hybridization of the interface $|\mathrm{i}\rangle$ and donor $|\mathrm{d}\rangle$ charge states in the flip-flop qubit basis states. If the hybridization is weak, e.g., $|\mathrm{g}\rangle \approx |\mathrm{d}\rangle$ and $|\mathrm{e}\rangle \approx |\mathrm{i}\rangle$, then the electron-phonon matrix elements, depicted as the dashed arrows in Fig. 2a of the main text, are strongly suppressed. The reason for that is that the electron-phonon interaction Hamiltonian $H_{\mathrm{eph,o}}$ is diagonal in the $|\mathrm{i}\rangle$, $|\mathrm{d}\rangle$ basis, as indicated by Eq. (12) of the main text. As a result, the relaxation rate is suppressed for weak hybridization.

The hybridization is significant in the vicinity of the ionization point $E_z - E_z^0 = 0$, in the electric-field range where the on-site energy difference $e(E_z - E_z^0)d$ between the sites i and d is smaller or comparable to the tunnel coupling V_{t}. For the parameters in Table I of the main text, this electric-field range is $E_z - E_z^0 \lesssim 1.6$ kV/m. To confirm this estimate, we plot the squared overlaps of the charge qubit ground state $|\mathrm{g}\rangle$ with donor $|\mathrm{d}\rangle$ and interface $|\mathrm{i}\rangle$ states as a function of electric field in Fig. S1a. The figure does confirm that hybridization occurs within an electric-field range of a few kV/m around the ionization point. Comparing the $0\,\mathrm{T} < B < 0.2\,\mathrm{T}$ range of Fig. 2b of the main text with Fig. S1a, one can see that this electric-field range of strong hybridization coincides with the electric-field range where the relaxation is the fastest.

In the vicinity of the working point, denoted by the white cross in Fig. 2b of the main text and Fig. S1b, another important ingredient governing the flip-flop relaxation rate is the hyperfine-induced mixing of the flip-flop qubit excited state $|\mathrm{g}{\uparrow}{\Downarrow}\rangle$ with $|\mathrm{e}{\downarrow}{\Uparrow}\rangle_0$, see the level diagram in Fig. 2a of the main text. The stronger this mixing, the faster the relaxation. This relation is confirmed by comparing the flip-flop relaxation rate shown in Fig. 2b of the main text, and Fig. S1b, where we plot the squared overlap $|\langle \mathrm{g}{\uparrow}{\Downarrow}|\mathrm{e}{\downarrow}{\Uparrow}\rangle_0|^2$ as a function of the electric and magnetic field.

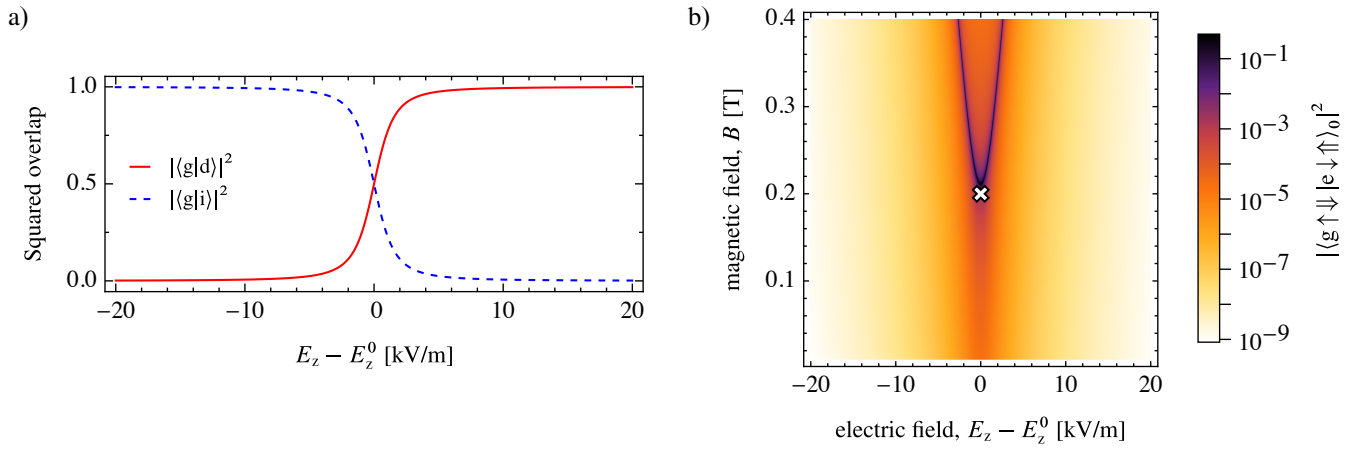

FIG. S1. (a) Squared overlaps $|\langle \mathrm{g}|\mathrm{d}\rangle|^2$ and $|\langle \mathrm{g}|\mathrm{i}\rangle|^2$ as functions of the electric field. We note that $|\langle \mathrm{g}|\mathrm{d}\rangle|^2 = |\langle \mathrm{e}|\mathrm{i}\rangle|^2$ and $|\langle \mathrm{g}|\mathrm{i}\rangle|^2 = |\langle \mathrm{e}|\mathrm{d}\rangle|^2$. (b) $|\langle \mathrm{g}{\uparrow}{\Downarrow}|\mathrm{e}{\downarrow}{\Uparrow}\rangle_0|^2$ as a function of the electric and magnetic field.

II. DERIVATION OF THE ELECTRON-PHONON HAMILTONIAN IN THE CHARGE-QUBIT HILBERT SPACE

A. Electron-phonon Hamiltonian

In silicon, the deformation-potential electron-phonon interaction is described by the Herring-Vogt Hamiltonian, which can be written as

$$H_{\rm eph} = H^{(d)}_{\rm eph} + H^{(u)}_{\rm eph}, \tag{S1}$$

where $H^{(d)}_{\rm eph}$, ($H^{(u)}_{\rm eph}$) is the deformation-potential Hamiltonian due to dilational (uniaxial) deformation. These terms have the forms

$$H^{(d)}_{\rm eph} = \Xi_d {\rm Tr}(\varepsilon) 1_{6\times 6}, \tag{S2a}$$

$$H^{(u)}_{\rm eph} = \Xi_u \begin{pmatrix} \varepsilon_{xx} & 0 & 0 & 0 & 0 & 0 \\ 0 & \varepsilon_{xx} & 0 & 0 & 0 & 0 \\ 0 & 0 & \varepsilon_{yy} & 0 & 0 & 0 \\ 0 & 0 & 0 & \varepsilon_{yy} & 0 & 0 \\ 0 & 0 & 0 & 0 & \varepsilon_{zz} & 0 \\ 0 & 0 & 0 & 0 & 0 & \varepsilon_{zz} \end{pmatrix}, \tag{S2b}$$

where Ξ_d, (Ξ_u) is the dilational (uniaxial) deformation potential, ε is the strain tensor and the 6×6 matrix structure corresponds to valley space which is denoted and ordered as $(x, \bar{x}, y, \bar{y}, z, \bar{z})$. Equations (S2a) and (S2b) show that the dilational and uniaxial terms have different structure in the valley space: the dilational term is valley-independent but the uniaxial term has a non-trivial valley dependence.

The diagonal elements of the strain tensor are given by Eq. (9) of the main text. The wave functions of the interface $|{\rm i}\rangle$ and donor $|{\rm d}\rangle$ states are given by Eq. (11) of the main text. To restrict the electron-phonon Hamiltonian $H_{\rm eph}$ to the charge-qubit Hilbert space we use the projection in Eq. (12) of the main text:

$$H_{\rm eph,o} = P H_{\rm eph} P, \tag{S3}$$

where $P = |{\rm i}\rangle\langle{\rm i}| + |{\rm d}\rangle\langle{\rm d}| = \sigma_0$ is the projector to the charge-qubit Hilbert space. To evaluate the right hand side of Eq. (S3), one has to calculate the following matrix elements:

$$\langle\sigma'|H_{\rm eph}|\sigma\rangle = \int {\rm d}\boldsymbol{r}\, \langle\sigma'|\boldsymbol{r}\rangle\, H_{\rm eph}\, \langle\boldsymbol{r}|\sigma\rangle\,, \tag{S4}$$

where $\sigma, \sigma' \in \{{\rm i}, {\rm d}\}$.

B. Electron-phonon Hamiltonian due to homogeneous deformation

As we argue in the main text, the plane-wave factor in Eq. (9) therein can be approximated by 1, yielding

$$\varepsilon^{(0)}_{jj} = i\sqrt{\frac{\hbar}{2\rho V}} \sum_{\boldsymbol{q},\lambda} \frac{e_{\boldsymbol{q}\lambda j} q_j}{\sqrt{v_\lambda q}} \left(a_{\boldsymbol{q},\lambda} + a^\dagger_{-\boldsymbol{q},\lambda}\right), \tag{S5}$$

which is independent of $\boldsymbol{r}$ and, accordingly, corresponds to a homogeneous deformation. From Eqs. (S2a) and (S2b), using the strain-tensor elements in Eq. (S5), we obtain the following expressions for the dilational and uniaxial electron-phonon Hamiltonians:

$$H^{(d,0)}_{\rm eph} = i\Xi_d \sqrt{\frac{\hbar}{2\rho V}} \sum_{\boldsymbol{q},\lambda} \frac{e_{\boldsymbol{q}\lambda x} q_x + e_{\boldsymbol{q}\lambda y} q_y + e_{\boldsymbol{q}\lambda y} q_y}{\sqrt{v_\lambda q}} 1_{6\times 6} \left(a_{\boldsymbol{q},\lambda} + a^\dagger_{-\boldsymbol{q},\lambda}\right), \tag{S6a}$$

$$H^{(u,0)}_{\rm eph} = i\Xi_u \sqrt{\frac{\hbar}{2\rho V}} \sum_{\boldsymbol{q},\lambda} \frac{1}{\sqrt{v_\lambda q}} \begin{pmatrix} e_{\boldsymbol{q}\lambda x} q_x & 0 & 0 & 0 & 0 & 0 \\ 0 & e_{\boldsymbol{q}\lambda x} q_x & 0 & 0 & 0 & 0 \\ 0 & 0 & e_{\boldsymbol{q}\lambda y} q_y & 0 & 0 & 0 \\ 0 & 0 & 0 & e_{\boldsymbol{q}\lambda y} q_y & 0 & 0 \\ 0 & 0 & 0 & 0 & e_{\boldsymbol{q}\lambda z} q_z & 0 \\ 0 & 0 & 0 & 0 & 0 & e_{\boldsymbol{q}\lambda z} q_z \end{pmatrix} \left(a_{\boldsymbol{q},\lambda} + a^\dagger_{-\boldsymbol{q},\lambda}\right). \tag{S6b}$$

The matrix elements defining the projected electron-phonon Hamiltonian $H_{\mathrm{eph,o}}$ in can be expressed using Eq. (S4) and the wave functions in Eq. (11) of the main text:

$$\langle \mathrm{i}|H_{\mathrm{eph}}^{(d,0)}|\mathrm{i}\rangle = \langle \mathrm{d}|H_{\mathrm{eph}}^{(d,0)}|\mathrm{d}\rangle = i\Xi_d\sqrt{\frac{\hbar}{2\rho V}}\sum_{\boldsymbol{q},\lambda}\frac{e_{\boldsymbol{q}\lambda x}q_x + e_{\boldsymbol{q}\lambda y}q_y + e_{\boldsymbol{q}\lambda z}q_z}{\sqrt{v_\lambda q}}\left(a_{\boldsymbol{q},\lambda} + a^\dagger_{-\boldsymbol{q},\lambda}\right), \tag{S7a}$$

$$\langle \mathrm{i}|H_{\mathrm{eph}}^{(u,0)}|\mathrm{i}\rangle = i\Xi_u\sqrt{\frac{\hbar}{2\rho V}}\sum_{\boldsymbol{q},\lambda}\frac{e_{\boldsymbol{q}\lambda z}q_z}{\sqrt{v_\lambda q}}\left(a_{\boldsymbol{q},\lambda} + a^\dagger_{-\boldsymbol{q},\lambda}\right), \tag{S7b}$$

$$\langle \mathrm{d}|H_{\mathrm{eph}}^{(u,0)}|\mathrm{d}\rangle = \frac{i\Xi_u}{3}\sqrt{\frac{\hbar}{2\rho V}}\sum_{\boldsymbol{q},\lambda}\frac{e_{\boldsymbol{q}\lambda x}q_x + e_{\boldsymbol{q}\lambda y}q_y + e_{\boldsymbol{q}\lambda z}q_z}{\sqrt{v_\lambda q}}\left(a_{\boldsymbol{q},\lambda} + a^\dagger_{-\boldsymbol{q},\lambda}\right). \tag{S7c}$$

The cross matrix elements between interface and donor states vanish.

Using the matrix elements obtained in Eq. (S7), the electron-phonon Hamiltonian in the charge-qubit Hilbert space can be written as

$$H_{\mathrm{eph,o}}^{(0)} = \underbrace{\frac{\langle \mathrm{i}|H_{\mathrm{eph}}^{(0)}|\mathrm{i}\rangle + \langle \mathrm{d}|H_{\mathrm{eph}}^{(0)}|\mathrm{d}\rangle}{2}}_{\Pi_0^{(0)}}\sigma_0 + \underbrace{\frac{\langle \mathrm{i}|H_{\mathrm{eph}}^{(0)}|\mathrm{i}\rangle - \langle \mathrm{d}|H_{\mathrm{eph}}^{(0)}|\mathrm{d}\rangle}{2}}_{\Pi_z^{(0)}}\sigma_z, \tag{S8}$$

where $\sigma_z = |\mathrm{i}\rangle\langle \mathrm{i}| - |\mathrm{d}\rangle\langle \mathrm{d}|$. The term proportional to σ_0 is not contributing to relaxation. The relevant factors read

$$\Pi_z^{(d,0)} = 0, \tag{S9a}$$

$$\Pi_z^{(u,0)} = \frac{i\Xi_u}{6}\sqrt{\frac{\hbar}{2\rho V}}\sum_{\boldsymbol{q},\lambda}\frac{-e_{\boldsymbol{q}\lambda x}q_x - e_{\boldsymbol{q}\lambda y}q_y + 2e_{\boldsymbol{q}\lambda z}q_z}{\sqrt{v_\lambda q}}\left(a_{\boldsymbol{q},\lambda} + a^\dagger_{-\boldsymbol{q},\lambda}\right). \tag{S9b}$$

Finally, the electron-phonon interaction Hamiltonian in the charge-qubit Hilbert space has the form

$$H_{\mathrm{eph,o}}^{(0)} = \frac{i\Xi_u}{6}\sqrt{\frac{\hbar}{2\rho V}}\sum_{\boldsymbol{q},\lambda}\frac{-e_{\boldsymbol{q}\lambda x}q_x - e_{\boldsymbol{q}\lambda y}q_y + 2e_{\boldsymbol{q}\lambda z}q_z}{\sqrt{v_\lambda q}}\left(a_{\boldsymbol{q},\lambda} + a^\dagger_{-\boldsymbol{q},\lambda}\right)\sigma_z, \tag{S10}$$

which is the result shown in Eq. (12) of the main text.

C. Changing the valley composition of the donor state can prolong the relaxation time

In the main text, we highlighted the fact that certain mechanisms can change the valley composition of the electronic ground state of the donor. Here, we quantify how such a valley repopulation affects the relaxation times.

We consider the case when the donor wave function has the form [to be compared with Eq. (11b) of the main text]

$$\langle \boldsymbol{r}|\mathrm{d}\rangle = \sqrt{\delta(\boldsymbol{r})}\frac{1}{\sqrt{2}}\left(\sqrt{\frac{1-P_z}{2}}, \sqrt{\frac{1-P_z}{2}}, \sqrt{\frac{1-P_z}{2}}, \sqrt{\frac{1-P_z}{2}}, \sqrt{P_z}, \sqrt{P_z}\right), \tag{S11}$$

where P_z characterizes the z-valley population of the donor electron. Increasing P_z from 1/3 to 1, the valley composition of the donor state turns from bulk-like to interface-like.

Repeating the calculation for the electron-phonon Hamiltonian due to homogeneous deformation using the wave function in Eq. (S11), we get

$$H_{\mathrm{eph,o}}^{(0)}(P_z) = \frac{3}{2}(1-P_z)H_{\mathrm{eph,o}}^{(0)}(P_z = 1/3), \tag{S12}$$

where $H_{\mathrm{eph,o}}^{(0)}(P_z = 1/3)$ equals to $H_{\mathrm{eph,o}}^{(0)}$ in Eq. (S10). Since the relaxation times are inversely proportional to the squared electron-phonon Hamiltonian's matrix elements, Eq. (S12) implies that for each (charge, flip-flop, spin) relaxation time it holds that

$$T_1(P_z) = \frac{4}{9(1-P_z)^2}T_1(P_z = 1/3). \tag{S13}$$

For the case reported in Ref. 48 of the main text, where the z-valley population of the donor ground state is estimated as $P_z = 40\%$, the relaxation time is increased by 23.5%.